Biochemistry

 Volume 39, Number 8 February 29, 2000

Accelerated Publications

Structure of Sterol Carrier Protein 2 at 1.8 Å Resolution Reveals a Hydrophobic Tunnel Suitable for Lipid Binding[†,‡]

Thomas Choinowski, Helmut Hauser, and Klaus Piontek*

Institute of Biochemistry, Swiss Federal Institute of Technology (ETH), Universitätstrasse 16, CH-8092 Zürich, Switzerland

Received November 30, 1999

ABSTRACT: Sterol carrier protein 2, also known as nonspecific lipid transfer protein is a ubiquitous, small, basic protein of 13 kDa found in animals. Its primary structure is highly conserved between different species, and it has been implicated in the intracellular transport of lipids and in a wide range of other in vitro functions related to sterol and fatty acid metabolism. Sterol carrier protein 2 deficiency in mice leads to elevated concentrations of phytanic acid in the serum and causes hepatocarcinogenesis. However, its actual physiological role is still unknown. Although sterol carrier protein 2 has been studied extensively in the past 20 years, very little is known concerning its three-dimensional structure. The crystal structure of rabbit sterol carrier protein 2, determined at 1.8 Å resolution with the MIRAS method, shows a unique α/β-fold. The core of this protein forms a five-stranded antiparallel β-sheet flanked by five helices. A C-terminal segment (residues 114−123), together with part of the β-sheet and four α-helices, form a hydrophobic tunnel providing the environment for apolar ligands such as fatty acids and fatty acyl-coenzyme As. Structurally well-characterized nonspecific lipid transfer proteins from plants have hydrophobic tunnel-like cavities, which were identified as the binding site for fatty acids and related apolar ligands. Despite the fact that plant nonspecific lipid transfer proteins are smaller proteins than sterol carrier protein 2, show no sequence homology to sterol carier protein 2, and are structurally unrelated, the cavities of these two classes of proteins are very similar with respect to size, shape, and hydrophobicity, suggesting a common functional role.

The intracellular sterol carrier protein 2 (SCP2)[1] is an animal nonspecific lipid transfer protein (nsLTP) of 13 kDa. It is a ubiquitous basic protein with a primary structure highly conserved in different species (*1*). SCP2 is encoded by a single gene that has two initiation sites (*2*). The translation products are two proteins: SCPx of 58 kDa and pre-SCP2 of 15 kDa. The 20 amino acid leader sequence of pre-SCP2 is rapidly cleaved after translation to yield the mature 13.2 kDa SCP2 (*2*). SCPx is a fusion protein containing a thiolase domain at the N-terminus and SCP2 at the C-terminus (*3*). SCP2 carries a C-terminal peroxisomal targeting signal (PTS1) and has been shown to be predominantly localized in peroxisomes (*4*), while SCPx occurs exclusively in peroxisomes, which are involved in the β-oxidation of fatty acids. Other proteins with C-terminal SCP2 domains are the

[†] This project was supported in part by Swiss National Science Foundation Grant 2-77-206-91 and Kamillo-Eisner Stiftung Grant 2-85-045-97.

[‡] Coordinates have been deposited with the Protein Data Bank, http://www.rcsb.org/pdb/, under code 1C44.

* Corresponding author: Institut für Biochemie, ETH-Zentrum, Universitätstrasse 16, CH-8092 Zürich, Switzerland. Telephone: ++41-1-632-3141. Fax: ++41-1-632-1121. E-mail: klaus.piontek@bc.biol.ethz.ch.

[1] Abbreviations: CoA, coenzyme A; f.o.m., figure of merit, MIRAS, muliple isomorphous replacement including anomalous scattering; nsLTP, nonspecific lipid transfer protein; SCP2, sterol carrier protein 2; PPARα, peroxisomal proliferator-activated receptor α; PTS1, peroxisomal targeting signal; rms, root-mean-square.

10.1021/bi992742e CCC: $19.00
Published on Web 02/04/2000

peroxisomal D-hydroxyacyl-CoA dehydrogenase and the *Caenorhabditis elegans* behavioral protein. It is assumed that in all these proteins SCP2 functions as a lipid binding domain.

SCP2 deficiency in mice was shown to cause peroxisome proliferation and severe impairment of the peroxisomal pathway involving the oxidation of α- and β-methylated acyl-CoA, leading to drastically elevated concentrations of phytanic acid in the serum and spontaneous hepatocarcinogenesis (*5*). The authors concluded that one function of SCP2 is the mediation of methyl-branched fatty acyl-CoA degradation in the peroxisomal pathway. Furthermore, SCP2 deficiency was found to be associated with chronic superstimulation of the peroxisomal proliferator-activated receptor α (PPARα) (*6*). PPARα, being a ligand-dependent transcription factor, participates in the regulation of peroxisome function and lipid metabolism at the level of gene transcription (*7*). One physiological ligand of PPARα is phytanic acid (*6*). This is of particular interest, since an accumulation of this fatty acid was not only found in SCP2 null mice but also in patients with several inherited diseases, e.g. Zellweger syndrome (*8*).

Since the discovery of SCP2 in 1968 (*9*), an ever increasing number of in vitro functions have emerged: SCP2 was shown to be involved in the esterification of free cholesterol, to activate the enzymatic conversion of 7-dehydrocholesterol to cholesterol (10), and the biosynthesis of bile acid and steroid hormones (*11*). SCP2 catalyzes the intermembrane transfer of cholesterol, phospholipids, and glycolipids (*12*). More recently, it was found that SCP2 binds in vitro long-chain fatty acids and long-chain fatty acyl-CoAs with K_d values in the μM and nM range, respectively (*13*−*15*). Together, with acyl-CoA binding protein and fatty acid binding protein, SCP2 appears to be a major determinant in controlling the concentration of free long-chain fatty acyl-CoA in the cytosol (*16*). In summary, from in vitro experiments, two different roles of SCP2 are proposed, one being that SCP2 functions as a lipid transfer protein, the other that SCP2 is a carrier for fatty acids, fatty acyl-CoAs, or sterols such as cholesterol.

Despite the wide range of in vitro functions, neither the actual physiological role(s) nor the mechanism of action of SCP2 is yet known. Very little, indeed, is known of the structure underlying these functions and of the binding mode with proposed ligands.

EXPERIMENTAL PROCEDURES

Protein Expression, Purification, Crystallization, and X-ray Data Collection. Recombinant rabbit SCP2 was obtained by overexpressing SCP2 in *Escherichia coli* (BL-21) and purifying the resulting protein to apparent electrophoretic homogeneity. The purification and crystallization of the protein as well as the crystallographic data collection of the native protein crystals were described previously (*17*). In brief, single crystals of SCP2 were obtained at 4 °C with the vapor diffusion method equilibrating a mixture of 5 μL reservoir solution (2.0 M ammonium sulfate, 300 mM lithium sulfate in 100 mM citrate buffer at pH = 6.5) and an equal volume of the protein solution (10 mg/mL protein, buffered in 10 mM Tris·HCl, pH = 7.0). Stabilization of the radiation-sensitive crystals were achieved by addition of 30% (w/v) sucrose to the crystallization medium and using cryo-conditions at 100 K. Heavy atom derivatives were prepared by soaking native crystals in the cryo solution for 30−40 min containing 10 mM of the heavy atom compounds CH_3HgCl and K_2PtCl_6. Diffraction data were collected at the EMBL outstation, DESY/Hamburg at beamline BW7B using a wavelength of 0.8345 Å and a MarResearch image plate. Data were processed and scaled (Table 1) by using the programs DENZO and SCALEPACK (*18*).

Table 1: X-ray Crystallography Data

	native	CH_3HgCl	K_2PtCl_6
data collection statistics			
resolution range (Å)	18−1.8	18−2.0	18−2.0
total observations	104 415	67 894	67 792
unique reflections	14 102	10 327	10 370
completeness (%)	99.9 (99.8)[a]	98.0 (98.5)	98.8 (99.7)
I/σ	35.6 (5.6)	15.5 (5.9)	18.9 (7.0)
R_{merge} (%)[b]	4.9	7.2	6.8
phasing statistics			
R_{iso} (%)[c]		22.6	30.0
number of sites		1	2
mean f. o. m.	0.57		
refinement statistics			
resolution range (Å)	10−1.8		
R value (%)[d]	17.5		
R_{free} (%)[e]	24.4		
total no. of atoms	1,096		
mean B-factors (Å^2)	32.1		
protein	30.1		
water molecules	45.8		
rms deviations (Å)			
bonds	0.017		
angles	0.032		

[a] Values in parentheses correspond to the highest resolution shell. [b] $R_{merge} = \sum_h\sum_i|\langle I(h)\rangle - I(h)_i|/\sum_h\sum_i I(h)_i$ where $I(h)$ is the intensity of reflection h, $\sum_h$ is the sum over all reflections and $\sum_i$ is the sum over all i measurements of reflection h. [c] $R_{iso} = \sum||F_{PH}| - |F_P||/\sum|F_P|$ where F_{PH} and F_P are the structure factors for the derivative and the native data, respectively. [d] R-factor $= \sum(|F_{obs}| - |F_{calc}|)/\sum|F_{obs}|$. [e] R_{free} is the R value calculated for a test set of reflections, comprising a randomly selected 5% of the data, which was not included during refinement.

Structure Solution and Refinement. The heavy atom positions were located by difference Patterson techniques, subsequently refined, and initial MIRAS (multiple isomorphous replacement including anomalous scattering) phases were calculated to 2.5 Å resolution for the two possible enantiomorphous space groups $P4_12_12$ and $P4_32_12$, using the program SOLVE (*19*). The choice of the correct space group was made based on the better figure of merits. The quality of the resulting electron density map was such that the immediate recognition of the five-stranded β-sheet was possible. No phase improvement methods were required to build an initial atomic model encompassing residues 8−88 and 98−113, which corresponds to 78% of the 123 amino acids of SCP2. Refinement of the initial structure with the program REFMAC from the program suite CCP4 (*20*) resulted in a first R-factor of 38.5% (R_{free} = 42.6%) in the 10−2.5 Å resolution range. During the initial stages of model-building, an automatic insertion of water molecules was followed with the program ARP (*21*). Chain-tracing and model-building were carried out with the program CHAIN (*22*). The stereochemistry of the final, refined model was examined by the PROCHECK program (*23*). To search for structural and folding similarities of SCP2 with proteins in the Protein Data Bank (http://www.rcsb.org/pdb/) the pro-

gram DALI (*24*) was used.

RESULTS

Structure Determination. The crystal structure of rabbit SCP2 was determined using the MIRAS-technique. Cubic-like crystals belonging to the tetragonal space group $P4_12_12$ with cell dimensions $a = b = 57.5$ Å and $c = 86.5$ Å could be grown to a size of $0.5 \times 0.5 \times 0.4$ mm^3 within 2−3 months. Calculations of the solvent content (*25*) suggested that one protein molecule is present in the asymmetric unit. The assignment of residues 6−113 to the electron density (Figure 1A) was straightforward, while the electron density of the C- and N-terminal segments was rather weak and thus model-building more difficult. Nevertheless, we succeeded in including amino acids 1−5 and 114−123, but these segments appeared to be rather mobile as judged by the high-temperature factors. A total of 140 water molecules were included in the structural model. The refined model has good stereochemistry (Table 1), and only one nonglycine residue, Gln115, present in a sharp turn of the C-terminal segment, was found in the disallowed region of the Ramachandran plot.

During the crystal structure determination, an error of the amino acid sequence was detected: residue 75, reported by Weber et al. (*26*) to be an isoleucine, was unambiguously assigned to a methionine from the electron densities of the MIRAS maps (Figure 1B) and omit $(nF_o - F_c)\exp(i\alpha_c)$ maps ($n = 1,2$) (Figure 1C) and was refined as such. This finding was confirmed by MALDI-MS of the protein (*17*), which showed that the experimentally determined molecular mass was only 1 Da different from the calculated mass, with methionine at position 75. The correctness of a methionine is further supported by a high conservation of this amino acid in all SCP2 sequences reported sofar. The amino acid error is due to a sequencing mistake of the rabbit small-intestinal cDNA clone (F. Weber, University of Zürich, personal communication).

Description of the Structure. The SCP2 molecule of an overall size of about $40 \times 25 \times 25$ Å^3 exhibits a unique α/β-fold. There is no similarity with any currently deposited protein in the Protein Data Bank. The basic structural element of SCP2 is a five-stranded β-sheet of a −1−1 3X 1 topology (Figure 2). Strands I−III and IV−V form two antiparallel sub sheets, with strands I and IV being parallel and strands III and IV being connected through a right-handed crossover chain (residues 65−69) traversing strands I and II on the backside of the β-sheet. Strand I is formed by residues Gly33−Lys40, strand II by Ala48−Val54, strand III by Ser60−Pro63, strand IV by Cys71−Ala76, and strand V by Lys100−Gly103. The front-side of the β-sheet, facing the reader (Figure 2), is dominated by hydrophobic residues, while the backside is mostly hydrophilic. On the front-side, the β-sheet is flanked on three edges by helices A−E. Most prominent is the long N-terminal α-helix A comprising residues Phe7−Glu22 on the left edge of the β-sheet. It is amphipathic with apolar residues oriented toward the hydrophobic surface of the β-sheet and polar residues facing the solvent region. The α-helix B (Glu23−Ile31), the 3_{10}-helix C (Gly42−Lys46), and α-helices D (Asp77−Phe85) and E (Asn89−Gln96) are all short consisting of only one to two turns. The C-terminal α-helix F (Asn104−Asn113)

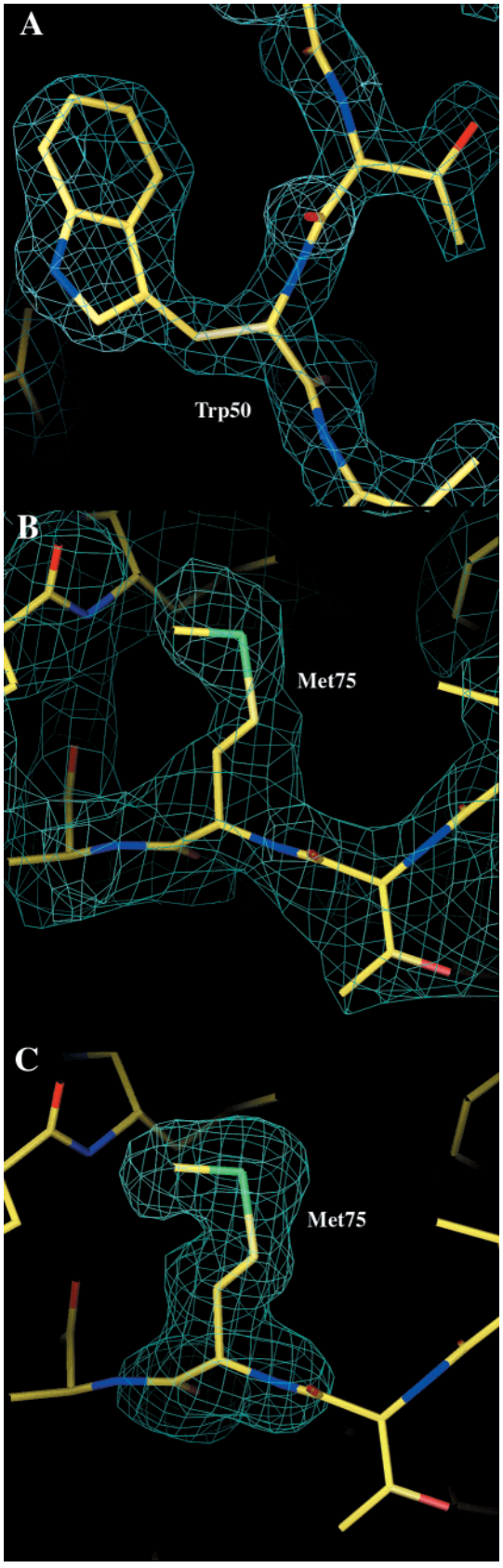

FIGURE 1: Electron density of SCP2. (A) A representative portion of the final $(2F_o - F_c)\exp(i\alpha_c)$ map around Trp50 at 1.8 Å resolution. (B) MIRAS map at position 75, calculated at 2.5 Å resolution. (C) Difference omit map for residue 75 at 1.8 Å resolution. The latter two maps show that residue 75 is a methionine rather than an isoleucine (see text). All maps are contoured on a 2σ level and were produced with "O" (*35*).

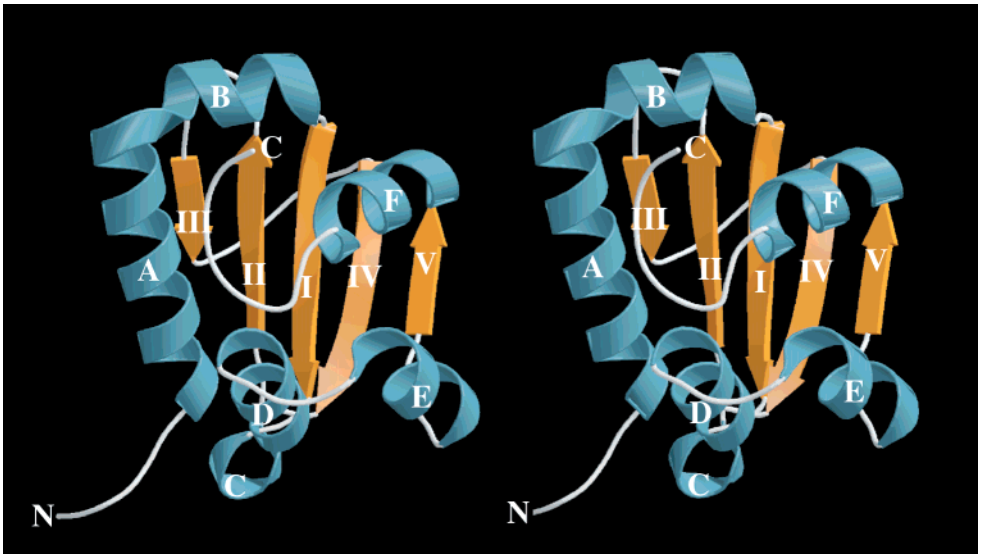

FIGURE 2: Stereoview of a ribbon diagram of SCP2 produced with MOLSCRIPT (*36*) and RASTER3D (*37*) showing helices in blue and β-strands in orange.

extends from the upper right edge toward the left edge of the β-sheet. The remaining N- and C-terminal residues lack a regular secondary structure. The C-terminal segment, first extending toward α-helix D and after making a sharp turn approaches α-helix B, has a few hydrophobic contacts to α-helices D and E. In contrast, the N-terminal peptide shows practically no interactions with the rest of the molecule. Residual electron density in the N- and C-terminal regions suggests that both terminal segments have some degree of static disorder and/or high-thermal flexibility. The structural assignment of these portions of the protein has, therefore, to be treated cautiously.

SCP2 is a basic protein with a calculated pI of 9.8 (*17*). The charge distribution of the protein shows that there are two clusters of basic amino acids, which may represent the putative binding site for the acidic part of ligands (Figure 3A and D), such as the carboxylate group of a fatty acid or the pyrophosphate group of a fatty acyl-CoA. Apart from these clusters, the rest of the charged residues of SCP2 appear to be evenly distributed over the hydrophilic back face of the β-sheet and over the hydrophilic surface of the amphipathic α-helices A and B, the bottom part of α-helix D, and connecting peptides between helices D and E and between helix E and β-strand V.

The front-side of the β-sheet and α-helices D, E, and F and the right edge of the protein (see Figure 2 and Figure 3, A and D) are predominantly uncharged, forming an extended hydrophobic region. Specifically, β-strands II, I, IV, and V, α-helices A, D, E, and F, the loop between helices D and E, and the C-terminal segment form a hydrophobic tunnel. The length of this tunnel is about 18 Å and has in most parts a diameter of 7−8 Å. Its entrance is built up by β-strand V and helices E and F (Figure 2 and Figure 3D). In Figure 3D, we look through the tunnel from the entrance-side and a view from the opposite direction is presented in Figure 3C. Figure 3D shows one cluster of positively charged residues on the right-hand side of the tunnel entrance, and the hydrophobic nature of the protein surface surrounding the entrance. The interior of the tunnel is almost completely hydrophobic with only one charged side chain of Lys120

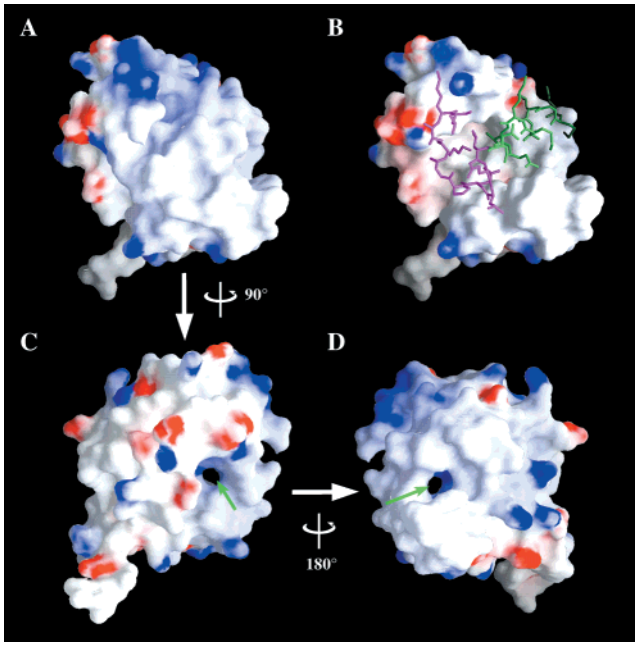

FIGURE 3: Electrostatic surface potential of SCP2 produced with the program GRASP (*38*) and RASTER3D (*37*). Negative surface potentials in red, positive surface potentials in blue, and neutral surface potentials in white. (A) The orientation of SCP2 is as in Figure 2. This side of the molecule is referred to as the front-side. (B) The orientation of SCP2 is the same as in (A), however, α-helix F (green) and the remaining C-terminal portion (magenta) are depicted as stick models. This representation was chosen to delineate the underlying topology of the hydrophobic surface of the tunnel interior. The orientation of SCP2 in (C) and (D) were obtained by a 90° anticlockwise rotation and a 90° clockwise rotation, respectively, of the molecule in (A) about a vertical axis in the plane of the paper. These representations reveal the proposed exit and entrance of the tunnel, respectively (see green arrows).

protruding into this channel. There is no evidence from the electron density for the presence of ordered water molecules in the interior of the hydrophobic cavity. The end of the tunnel lies between α-helix A and the C-terminal segment (Figure 2 and Figure 3C).

The shape of SCP2 may be approximated by an open right-hand where the ring and middle finger represent the β-sheet,

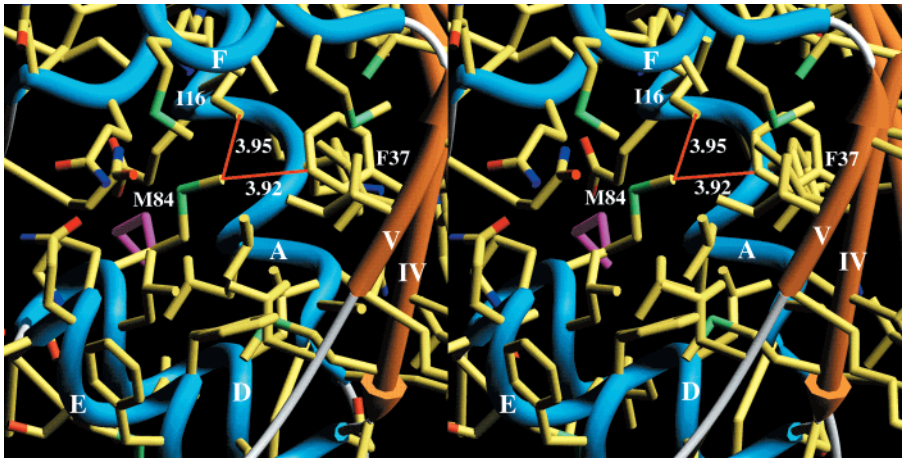

FIGURE 4: Stereoview of the hydrophobic tunnel of SCP2 depicted as combined ribbon-stick model. Helices (cyan) are labeled with capital letters and β-strands (orange) with Roman numbers as in Figure 2. The red lines represent the closest distances (Å) between residues Met84 and Phe37 and Met84 and Ile16, respectively, which form a narrow part in the tunnel. The side chain of Met84 shown in magenta is an alternative conformation in which the constriction of the tunnel is removed (see text). The image was produced with SETOR (39).

the small finger the α-helix A, the thumb together with the palm of the hand helices C, D, and E, and the forefinger bent toward the thumb helix F and the C-terminal segment. In this simplified picture, the thumb and forefinger would form the entrance of the hydrophobic tunnel.

The crystal structure presented here represents the first complete atomic model of an animal nsLTP. Previously, Szyperski and co-workers (*27*) reported a NMR-determination of the polypeptide fold of human SCP2 for residues 8−103. Basically, our structure determination confirms their assignment of the secondary structure elements, except that helices C, E, and F were not defined in the NMR model.

DISCUSSION

A Hydrophobic Tunnel as the Putative Substrate-Binding Site. From a functional point of view, the most interesting feature found in the three-dimensional crystal structure of SCP2 is the tunnel-like cavity lined by largely hydrophobic amino acids, thus providing the chemical environment for the binding of lipidic ligands. The length of this cavity is adequate to accommodate at least 16 carbon atoms. There is one constriction site within the tunnel where the diameter is reduced to about 4 Å. Thus, it appears that the insertion of an aliphatic chain is not possible (Figure 4). This narrow part of the tunnel is created by the close juxtaposition of the side chains of Phe37 and Met84 and Ile16 and Met84 located close to the end of the hydrophobic tunnel. Simple modeling shows that the side chain of Met84 can switch to another energetically favorable conformation without causing any steric conflict with other parts of the protein, thus increasing the width of the tunnel at this site to about 6 Å (Figure 4).

A hydrophobic area in the vicinity of the tunnel entrance is clearly seen in Figure 3D. Starting from the entrance of the tunnel, there is a narrow groove connecting the entrance with the cluster of three basic residues. Assuming that a fatty acid ligand enters the tunnel with its methyl end at this side, a portion of the aliphatic chain would snugly fit into this groove on the outside of the tunnel, with the carboxylate group of the fatty acid or the pyrophosphate group of a fatty acyl-CoA interacting with the basic residues.

Our proposal of the lipid-binding site in SCP2 is at least partly supported by reports in the literature. Site-directed mutagenesis experiments suggest that Asn104, the first residue of α-helix F, plays an important role in lipid binding (*2*). Other investigators reported that fatty acids are bound to SCP2 with their methyl end buried in the protein interior and their carboxylate exposed at the surface (*15*). Furthermore, evidence from fluorescence resonance energy transfer experiments (*28*) indicated that fatty acids bound to SCP2 are close to the single Trp50 in SCP2. Trp50 located in the β-strand II is part of the hydrophobic surface of the β-sheet in the vicinity of the proposed end of the tunnel between helix A and the C-terminal segment.

Comparison to Other Lipid-transfer Proteins. Presently, no tertiary structure of other animal nsLTPs is available for comparison. However, the crystal structure of SCP2 may be compared to the X-ray and NMR structures of the 9 kDa lipid-exchange proteins reported for the nsLTPs of wheat (*29*), barley (*30*), maize (*31*), and rice (*32*), and complexes of these proteins with ligands such as free fatty acid and fatty acyl-CoA. Although no sequence homology exists between SCP2 and the plant nsLTPs, and the folding motifs are different in the two classes of proteins, the examination of these structures in terms of the ligand-binding site topology is warranted. The fold of the plant proteins is characterized by four α-helices, short interconnecting loops, and a large C-terminal segment. The arrangement of the four helices and the large C-terminal segment is such that a hydrophobic tunnel-like cavity is formed of dimensions similar to that of SCP2. The extended C-terminal peptide chain functions as a lid covering the cavity where long-chain fatty acids can bind. In this binding mode, the carboxylate of the fatty acid is in contact with the solvent (*29*, *30*). There is practically no conformational change upon binding of palmitate (*33*), although there are reports that the hydrophobic cavity can slightly expand in order to accommodate larger lipid ligands (*34*) and that the actual size of the tunnel varies in proteins of different origin (*32*).

Liberation of the Peroxisomal Sequence upon Ligand Binding. Helix F contributing to the upper boundary of the putative ligand-binding tunnel forms only two hydrogen bonds (one involving Asn104, the other Gln112) and two well defined hydrophobic contacts with the core of the protein and as mentioned above the C-terminal peptide has

only a few weak hydrophobic interactions. When an aliphatic ligand enters the tunnel, it is feasible that helix F and the C-terminal segment move in order to accommodate the ligand. In this way, the diameter of the tunnel is increased and this mechanism would account for the observation that SCP2 can bind and apparently accommodate ligands of different sizes. The hinge that would allow for such a movement is probably located in the turn region between β-strand V and helix F. If such a movement occurs, then the weak hydrophobic interactions of the C-terminal segment are disrupted, and as a result, this segment may now extend into the solvent region. In this way, the peroxisomal targeting signal, the C-terminal tripeptide Ala-Lys-Leu, might become exposed, thus effecting the targeting of the SCP2−ligand complex to the PTS1 receptor. Such ligand-mediated protein targeting would represent a novel mechanism of cellular regulation. To support this hypothesis by structural data, we have initiated crystallization experiments of complexes of SCP2 with either long-chain fatty acids or fatty acyl-CoA. So far, all attempts to crystallize such complexes failed. One possible reason for this could be the anticipated release of the C-terminal segment from the core protein upon ligand binding. This loose end extending from the protein could sterically inhibit crystal contacts. We are currently engaged in producing SCP2 constructs with a slightly shortened C-terminus. Provided these modified SCP2 molecules still bind fatty acids strongly, crystallization experiments will be done in the presence of fatty acid ligands with the aim of obtaining protein−ligand complexes.

The putative ligand binding site of SCP2 apparently shares a number of features with the tunnel-like cavity of plant nsLTPs supporting the mode of ligand binding proposed here for SCP2 and suggesting a common functional role. The elucidation of the actual mode(s) of ligand binding to SCP2 will have to await the structure determination of ligand complexes.

ACKNOWLEDGMENT

We gratefully acknowledge the opportunity to collect diffraction data at the EMBL Outstation (DESY/Hamburg) and at the Swiss Norwegian Beamline (ESRF/Grenoble). We are indebted to Drs Wolfgang Welte and Kay Diederichs of the University of Konstanz (Germany) for allowing us to collect preliminary diffraction data on their rotating anode.

REFERENCES

1. Myers-Payne, S. C., Fontaine, R. N., Loeffler, A., Pu, L., Rao, A. M., Kier, A. B., Wood, W. G., and Schroeder, F. (1996) *J. Neurochem. 66*, 313−320.
2. Seedorf, U., Scheck, S., Engel, T., Steif, C., Hinz, H. J., and Assmann, G. (1994) *J. Biol. Chem. 269*, 2613−2618.
3. Ossendorp, B. C., van Heusden, G. P. H., de Beer, A. L. J., Bos, K., Schouten, G. L., and Wirtz, K. W. A. (1991) *Eur. J. Biochem. 201*, 233−239.
4. Ossendorp, B. C., and Wirtz, K. W. A. (1993) *Biochimie 75*, 191−200.
5. Seedorf, U., Raabe, M., Ellinghaus, P., Kannenberg, F., Fobker, M., Engel, T., Denis, S., Wouters, F., Wirtz, K. W., Wanders, R. J., Maeda, N., and Assmann, G. (1998) *Genes Dev. 12*, 1189−1201.
6. Ellinghaus, P., Wolfum, C., Assmann, G., Spener, F., and Seedorf, U. (1999) *J. Biol. Chem. 274*, 2766−2772.
7. Lemberger, T., Desvergne, B., and Wahli, W. (1996) *Annu. Rev. Cell. Dev. Biol. 12*, 335−363.
8. Steinberger, D. (1995) in *The Metabolic and Molecular Basis of Inherited Disease* (Scriver, C. R., Beaudet, A. L., Sly, W. S., and Valle, D., Ed.) pp 2351−2370, McGraw-Hill, New York.
9. Wirtz, K. W. A., and Zilversmit, D. B. (1968) *J. Biol. Chem. 243*, 3596−3602.
10. Noland, B. J., Arebalo, R. E., Hansbury, E., and Scallen, T. J. (1980) *J. Biol. Chem. 255*, 4282−4289.
11. Pfeifer, S. M., Furth, E. E., Ohba, T., Chang, Y. J., Rennert, H., Sakuragi, N., Billheimer, J. T., and Strauss, J. F. I. (1993) *J. Steroid Biochem. Mol. Biol. 47*, 167−172.
12. Zilversmit, D. B. (1984) *J. Lipid Res. 25*, 1563−1569.
13. Schroeder, F., Myers-Payne, S. C., Billheimer, J. T., and Wood, W. G. (1995) *Biochemistry 34*, 11919−11927.
14. Frolov, A., Cho, T. H., Billheimer, J. T., and Schroeder, F. (1996) *J. Biol. Chem. 271*, 31878−31884.
15. Stolowich, N. J., Frolov, A., Atshaves, B., Murphy, E. J., Jolly, C. A., Billheimer, J. T., Scott, A. I., and Schroeder, F. (1997) *Biochemistry 36*, 1719−1729.
16. Knudsen, J., Jensen, M. V., Hansen, J. K., Faergeman, N. J., Neergaard, T. B., and Gaigg, B. (1999) *Mol. Cell. Biochem. 192*, 95−103.
17. Choinowski, T., Dyer, J. H., Maderegger, B., Winterhalter, K. H., Hauser, H., and Piontek, K. (1999) *Acta Crystallogr. D 55*, 1478−1480.
18. Otwinowski, Z., and Minor, W. (1997) *Methods Enzymol. 276*, 307−326.
19. Terwilliger, T. C., and Berendzen, J. (1997) *Acta Crystallogr. D 53*, 571−579.
20. Collaborative Computing Project, Number 4 (1994) *Acta Crystallogr. D 50*, 760−763.
21. Lamzin, V. S., and Wilson, K. S. (1993) *Acta Crystallogr. D 49*, 129−147.
22. Sack, J. S. (1988) *J. Mol. Graphics 6*, 224−225.
23. Laskowski, R. A., MacArthur, M. W., Moss, D. S., and Thornton, J. M. (1993) *J. Appl. Crystallogr. 26*, 283−291.
24. Holm, L., and Sander, C. (1998) *Nucleic Acids Res. 26*, 316−319.
25. Matthews, B. W. (1968) *J. Mol. Biol. 33*, 491−497.
26. Weber, F. E., Dyer, J. H., Lopez, G. F., Werder, M., Szyperski, T., Wüthrich, K., and Hauser, H. (1998) *Cell. Mol. Life Sci. 54*, 751−759.
27. Szyperski, T., Scheek, S., Johansson, J., Assmann, G., Seedorf, U., and Wüthrich, K. (1993) *FEBS-Lett. 335*, 18−26.
28. Dansen, T. B., Westerman, J., Wouters, F. S., Wanders, R. J. A., van Hoek, A., Gadella, T. W. J., and Wirtz, K. W. A. (1999) *Biochem. J. 339*, 193−199.
29. Gincel, E., Simmore, J. P., Caille, P., Marion, D., Ptak, M., and Vovelle, F. (1994) *Eur. J. Biochem. 226*, 413−422.
30. Heinemann, B., Anderson, K. V., Nielsen, P. R., Bech, L. M., and Poulsen, F. M. (1996) *Protein Sci. 5*, 13−23.
31. Gomar, J., Petit, M. C., Sodano, P., Sy, D., Marion, D., Kader, J. C., Vovelle, F., and Ptak, M. (1996) *Protein Sci. 5*, 565−577.
32. Lee, J. Y., Min, K., Cha, H., Shin, D. H., Hwang, K. Y., and Suh, S. W. (1998) *J. Mol. Biol. 276*, 437−448.
33. Shin, D. H., Lee, J. Y., Hwang, K. Y., Kim, K. K., and Suh, S. W. (1995) *Structure 3*, 189−199.
34. Lerche, M. H. Kragelund, B. B., Bech, L. M., and Poulsen, F. M. (1997) *Structure 5*, 291−306.
35. Jones, T. A., Zou, J.-Y., Cowan, S. W., and Kjeldgaard, M. (1991) *Acta Crystallogr. A 47*, 110−119.
36. Kraulis, P. J. (1991) *J. Appl. Crystallogr. 24*, 946−950.
37. Merritt, E. A., and Bacon, D. J. (1997) *Methods Enzymol. 277*, 505−524.
38. Nicholls, A., Sharp, K., and Honig, B. (1991) *Proteins 11*, 281−296.
39. Evans, S. V. (1993) *J. Mol. Graphics 11*, 134−138.

BI992742E